

Supplementary Materials for

Chloride Sensing by WNK1 Involves Inhibition of Autophosphorylation

Alexander T. Piala, Thomas M. Moon, Radha Akella, Haixia He, Melanie H. Cobb,
Elizabeth J. Goldsmith*

*Corresponding author. E-mail: elizabeth.goldsmith@utsouthwestern.edu

Published 6 May 2014, *Sci. Signal.* **7**, ra41 (2014)

DOI: 10.1126/scisignal.2005050

The PDF file includes:

Fig. S1. Raw trace of WNK1-KDm/S* DSF using SYPRO Orange.

Fig. S2. Control kinase stability as a function of salt concentration.

Fig. S3. Phosphorylation of OSR1 by WNK1-KDm/S*.

Fig. S4. WNK1 autophosphorylation measured by mass spectrometry.

Fig. S5. Interaction of bound chloride with hydrophobic residues.

Table S1. Data and refinement statistics for WNK1-sKDm/S*.

Table S2. *B*-factors of the 3/10 helix residues in WNK1-KDm/SA and WNK1-sKDm/S*.

Table S3. Phosphorylation state of WNK1-KDm/S* mutants after purification from *E. coli*.

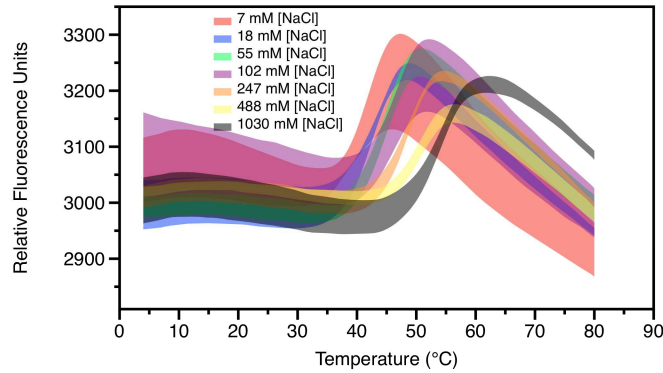


Fig. S1. Raw trace of WNK1-KDm/S* DSF using SYPRO Orange. Each curve represents three independent experiments, with the width of the curve representing one standard error above and below the mean.

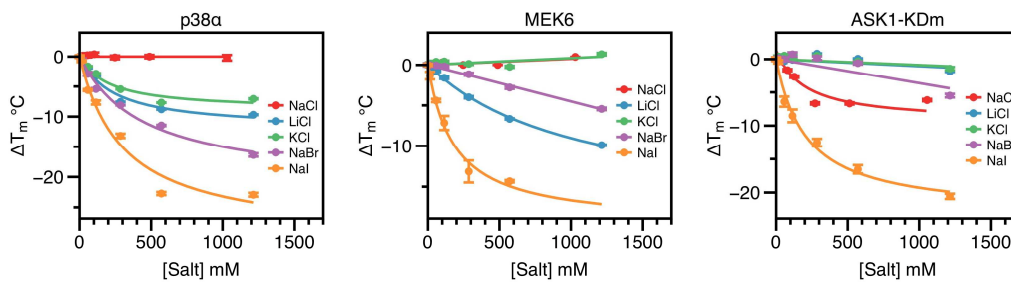


Fig. S2. Control kinase stability as a function of salt concentration. The indicated kinases or kinase catalytic domain were exposed to varying salt concentrations and their T_m was determined, as in Fig. 1A. Error bars represent standard error from three independent experiments.

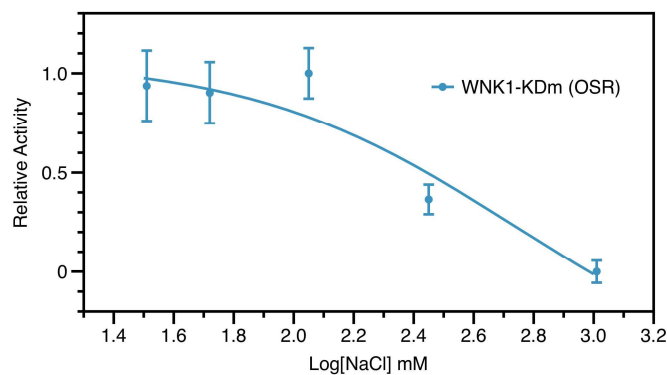


Fig. S3. Phosphorylation of OSR1 by WNK1-KDm/S*. Activity of WNK1 as measured by incorporation of ^{32}P into OSR1 (residues 1-295) as a function of $[\text{NaCl}]$. The highest measured activity was normalized to 1, and a control reaction in the absence of OSR was set as 0. Error bars represent standard error from three independent experiments.

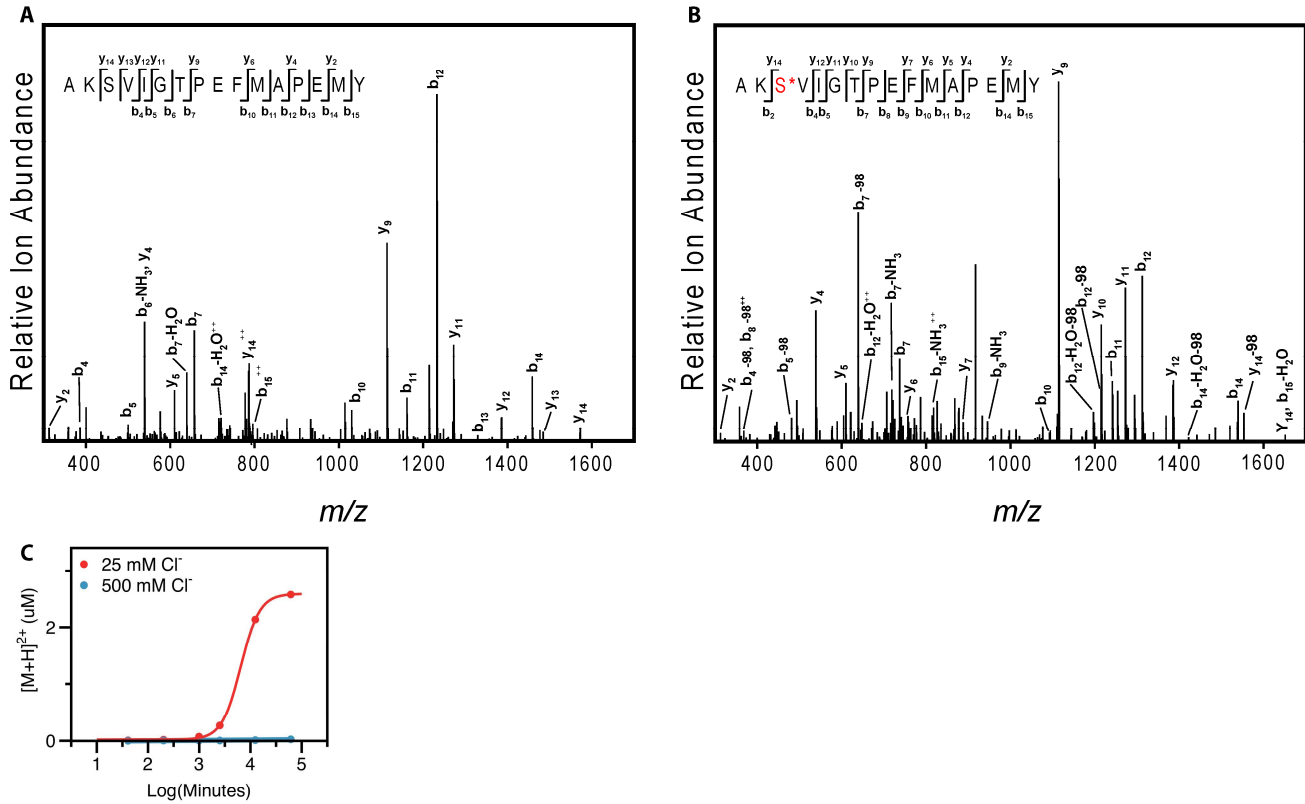


Fig. S4. WNK1 autophosphorylation measured by mass spectrometry. WNK1 chymotrypsin-derived activation loop peptides were identified by liquid-chromatography/mass-spectrometry (LC/MS/MS). (A) Unphosphorylated and (B) phosphorylated peptides at Ser³⁸² were identified by fragmentation analysis using MASCOT and by co-elution with known peptide standards. (C) Time courses for WNK1 in vitro autophosphorylation at Ser³⁸² were conducted in high (blue) and low (red) (500 mM and 25 mM, respectively) chloride concentrations. The higher concentration of Cl⁻ produced essentially no autophosphorylation.

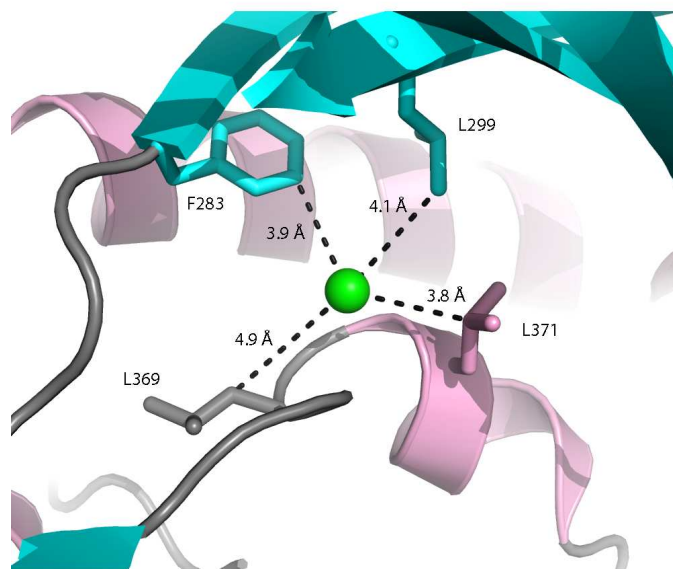


Fig. S5. Interaction of bound chloride with hydrophobic residues. The chloride ion in WNK1-KDm/SA makes Van-der-Walls contacts with F283, L299, and L371.

Table S1: Data and refinement statistics for WNK1-sKDm/S*.

WNK1-sKDm/S* (209-483)	
Space Group	P 1 2 ₁ 1
Unit Cell	$a=44.7 \text{ \AA}$, $b=64.2 \text{ \AA}$ $c=42.1 \text{ \AA}$, $\beta=92^\circ$
Resolution (\AA)	35-1.8 (1.7-1.8) [†]
Observed Reflections	75,996
Unique Reflections	19,568
Completeness	99.4 (98.8)
I/σ_I	30.5 (2.5)
Redundancy	3.7 (3.4)
$R_{work}(\%)$ [‡]	22.9
$R_{free}(\%)$	27.4
$R_{merge}(\%)$ [†]	0.051 (0.290)
Number of groups	
Protein Atoms	2215
Water	236
RMSD	
Bond Length, \AA	0.009
Bond Angle, $^\circ$	1.4
Average B factor, \AA^2	30.9
Ramachandran Map (%)	
Favorable	94.5
Allowed	5.1
Disallowed	0.4

[†] Values in Parentheses indicate the highest resolution shell

[‡] $R_{work} = \sum ||F_{obs} - F_{calc}|| / \sum |F_{obs}|$, where F_{obs} and F_{calc} are the observed and calculated structure factors, respectively.

Table S2. B-factors of the 3/10 helix residues in WNK1-KDm/SA and WNK1-sKDm/S*. Average residue B-factors are indicated.

Residue Number (C α)	B-Factor (\AA^2)	
	WNK1-KDm/SA (3FPQ Re-refinement)	WNK1-sKDm/S* (Phosphorylated WNK1)
365	15	15
366	12	15
367	14	18
368	18	25
369	19	30
370	20	39
371	22	40
372	22	45
373	22	52
374	25	66

Table S3: Phosphorylation state of WNK1-KDm/S* mutants after purification from *E. coli*.

WNK1-KDm/S* Mutant	Ser ³⁸² Phosphorylation (%)
WNK1-KDm/S* L299F	100
WNK1-KDm/S* L369F	84
WNK1-KDm/S* L371F	80